

Supporting Information for

**Solvent-Polymer Guest Exchange in Carbamazepine Inclusion
Complex: Structure, Kinetics and Implication for Guest
Selection**

Zhi Zhong,^a Xiaotong Yang,^a Bi-Heng Wang,^b Ye-Feng Yao,^b Baohua Guo,^a Lian Yu,^{*c}

Yanbin Huang^{*a} and Jun Xu^{*a}

^a Key Laboratory of Advanced Materials (MOE), Department of Chemical Engineering, Tsinghua University, Beijing 100084, China; Email: jun-xu@tsinghua.edu.cn (J. X.), and yanbin@tsinghua.edu.cn (Y. H.)

^b Physics Department and Shanghai Key Laboratory of Magnetic Resonance, School of Physics and Materials Science, East China Normal University, Shanghai 200062, China

^c School of Pharmacy and Department of Chemistry, University of Wisconsin-Madison, Madison, Wisconsin 53705, USA; Email: lian.yu@wisc.edu

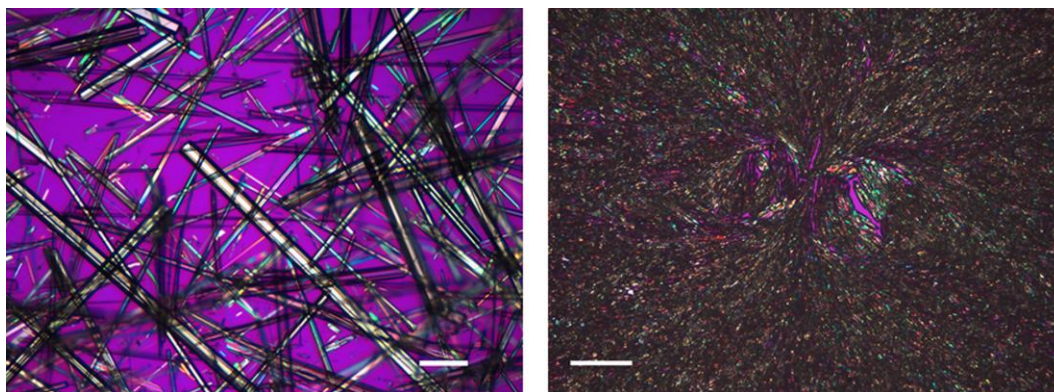


Fig. S1 POM images showing the crystal morphology of (left) CBZ Form II (toluene) grown from toluene solution and (right) CBZ Form II (PTHF) grown from 50 wt% CBZ/PTHF melt. The distinctly different crystal morphologies indicate the different preferred orientations. The bars represent 200 μm (left) and 100 μm (right), respectively.

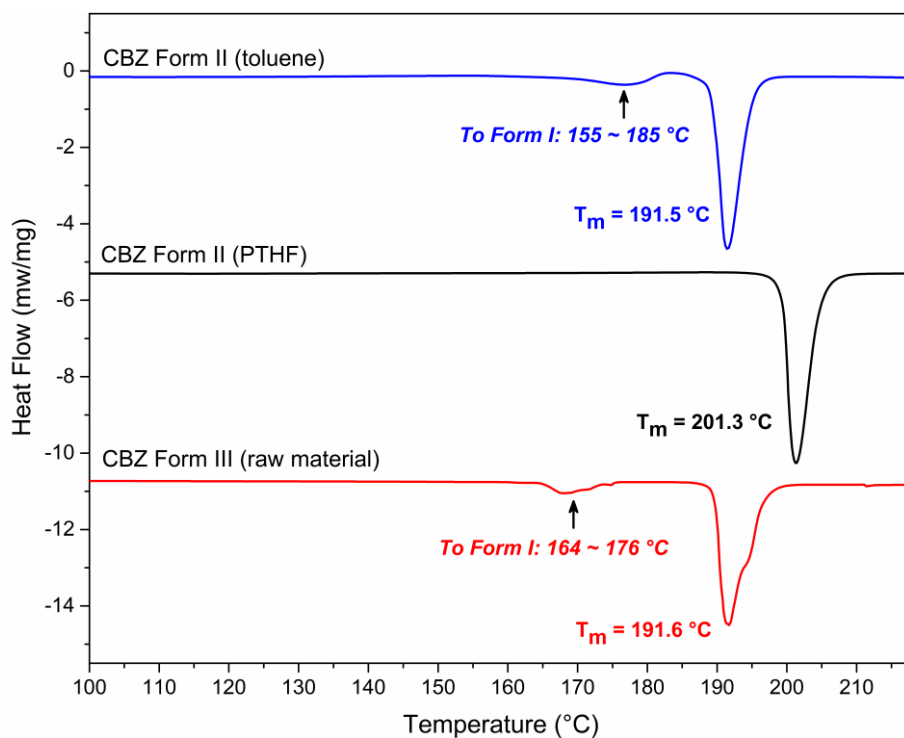
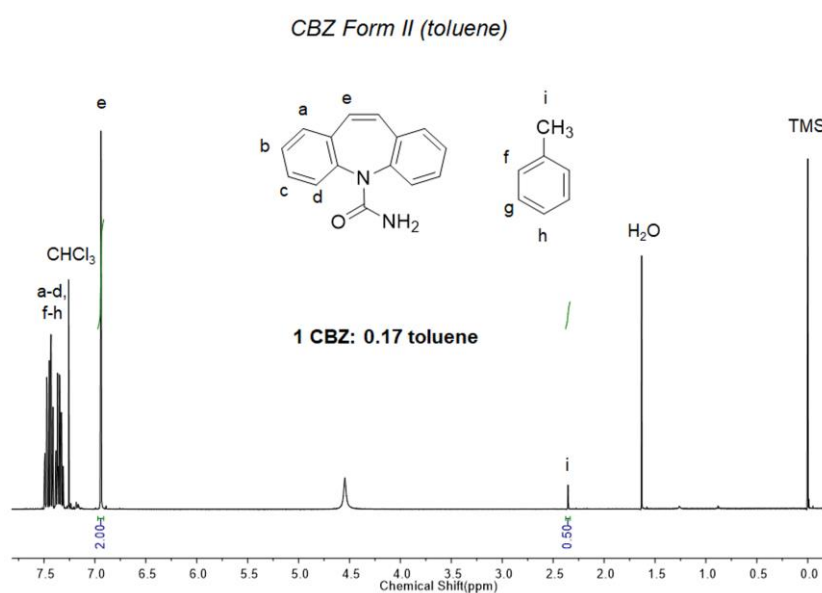


Fig. S2 DSC thermograms (from top to bottom) of CBZ Form II (toluene), CBZ Form II (PTHF) and CBZ Form III (raw material) at a heating rate of 10 °C/min. The weak endotherm between 155 and 185 °C for CBZ Form II (toluene) is attributed to the solvent release and conversion to CBZ Form I which is stable at high temperatures. The generated CBZ Form I then melted associated with a sharp endothermic peak around 191.5 °C. CBZ Form II (PTHF) showed no thermal events before the single sharp endothermic peak at about 201.3 °C due to melting. CBZ Form III (raw material) also transformed to CBZ Form I during the heating scan in the temperature range of 164 to 176 °C.



(a)

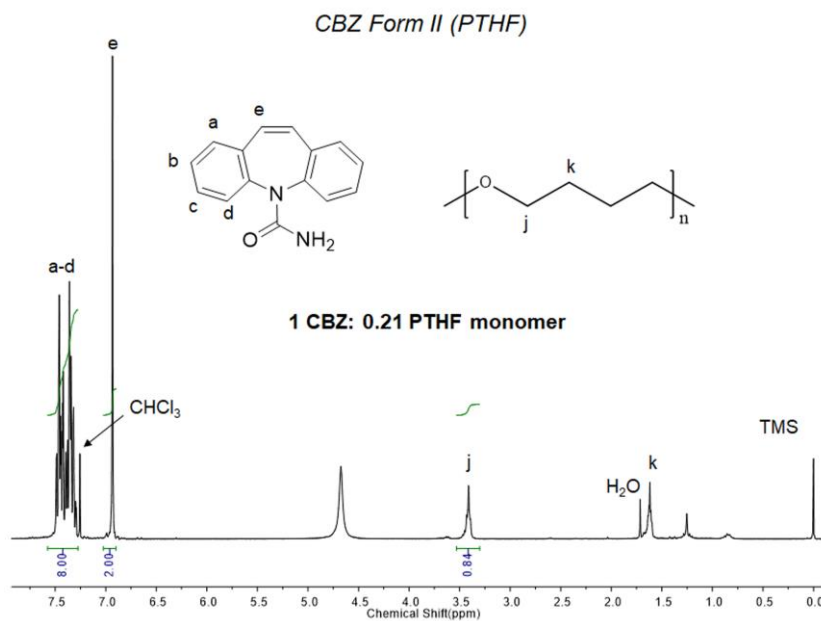


Fig. S3 $^1\text{H-NMR}$ spectra of (a) CBZ Form II (toluene) and (b) CBZ Form II (PTHF). CDCl_3 was used as the solvent. Characteristic signals of the different protons in CBZ, toluene and PTHF are marked with corresponding letters. The stoichiometric ratios of CBZ:toluene and CBZ:PTHF monomer were calculated using the integral area of the characteristic peaks.

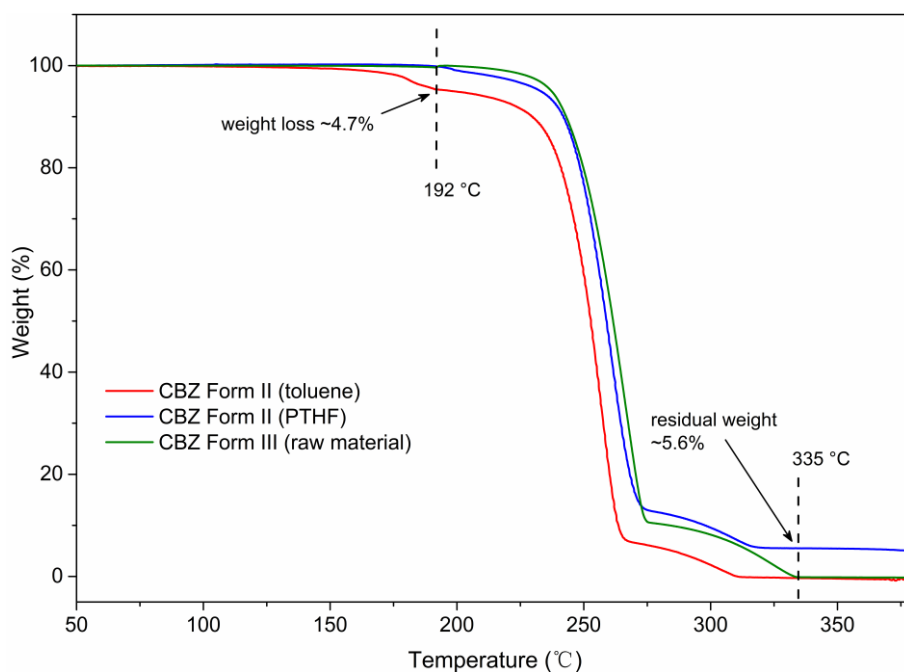
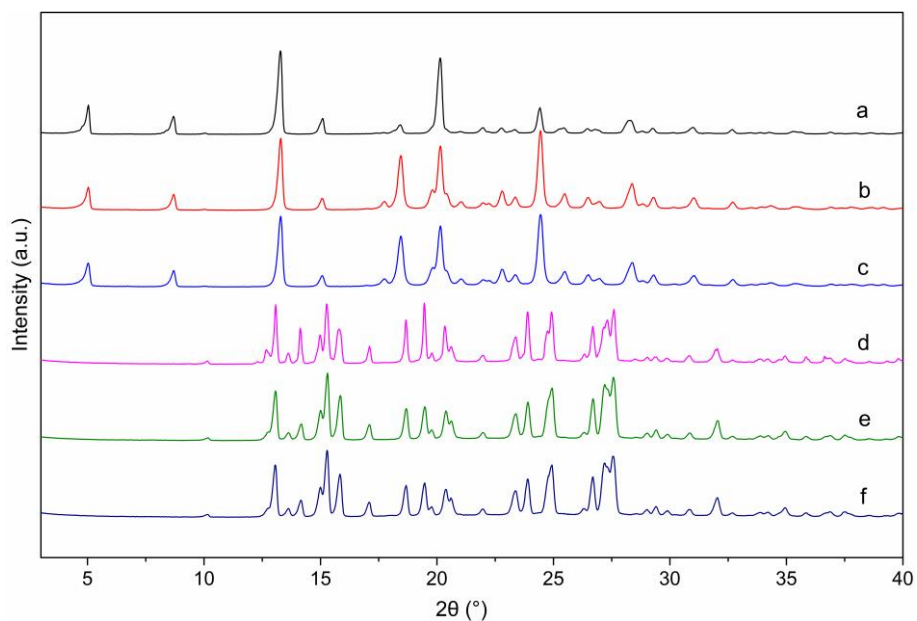
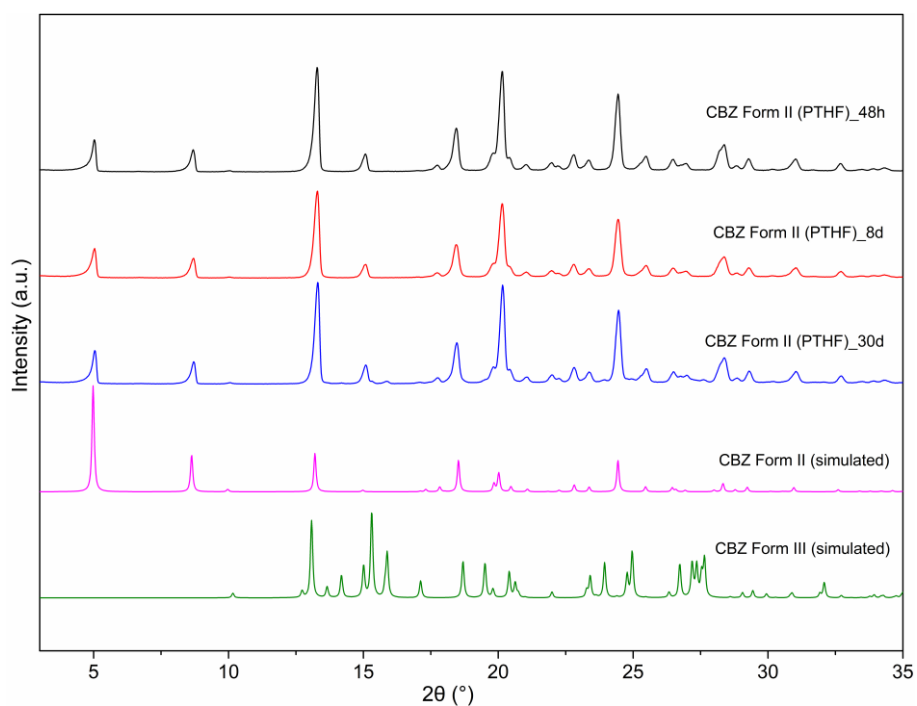


Fig. S4 TGA thermograms (from top to bottom) of CBZ Form II (toluene), CBZ Form II (PTHF) and CBZ Form III (raw material). The weight loss (~ 4.7 wt%) before $192\text{ }^\circ\text{C}$ for CBZ Form II (toluene) was associated with the solvent release, which was not detected for CBZ Form II (PTHF) and CBZ Form III. At $335\text{ }^\circ\text{C}$ when almost all CBZ molecules were lost, there was still $\sim 5.6\%$ of

the initial weight remaining, which should correspond with the guest PTHF.



(a)



(b)

Fig. S5 (a) PXR D patterns of CBZ Form II (PTHF) and CBZ Form III before and after equilibrium solubility test: *a.* initial CBZ Form II (PTHF); *b.* CBZ Form II (PTHF) after solubility test ($C_{\text{PTHF}} = 12 \text{ mg/mL}$); *c.* CBZ Form II (PTHF) after solubility test ($C_{\text{PTHF}} = 0 \text{ mg/mL}$); *d.* initial CBZ Form III; *e.* CBZ Form III after solubility test ($C_{\text{PTHF}} = 12 \text{ mg/mL}$); *f.* CBZ Form III after solubility test ($C_{\text{PTHF}} = 0 \text{ mg/mL}$). (b) PXR D patterns of CBZ Form II (PTHF) after suspending in toluene for different times. Only tiny amounts of CBZ Form III can be observed after 30 days, indicating the

long-term stability of CBZ Form II (PTHF) in toluene.

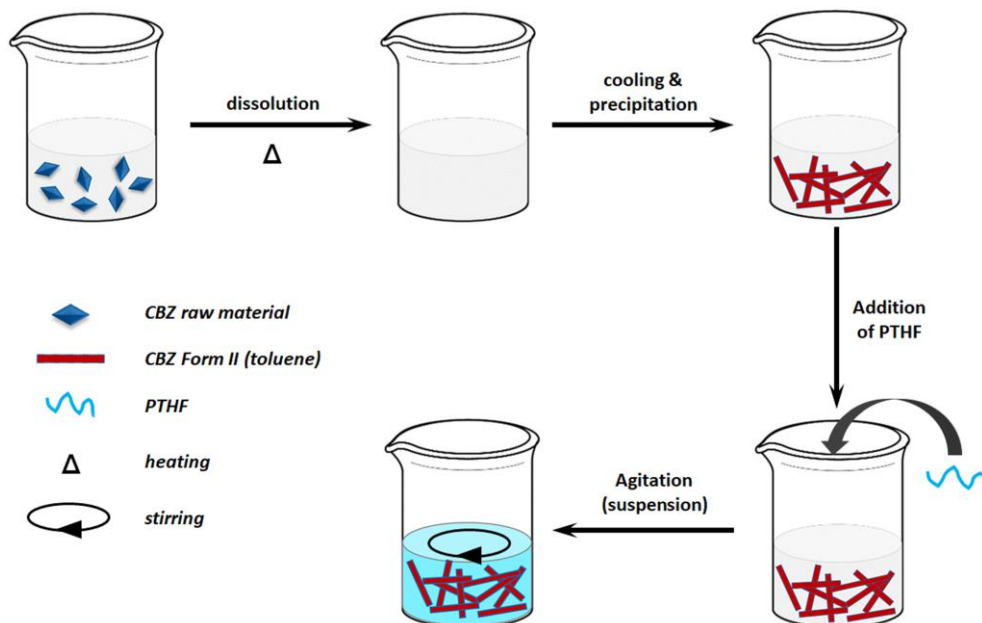
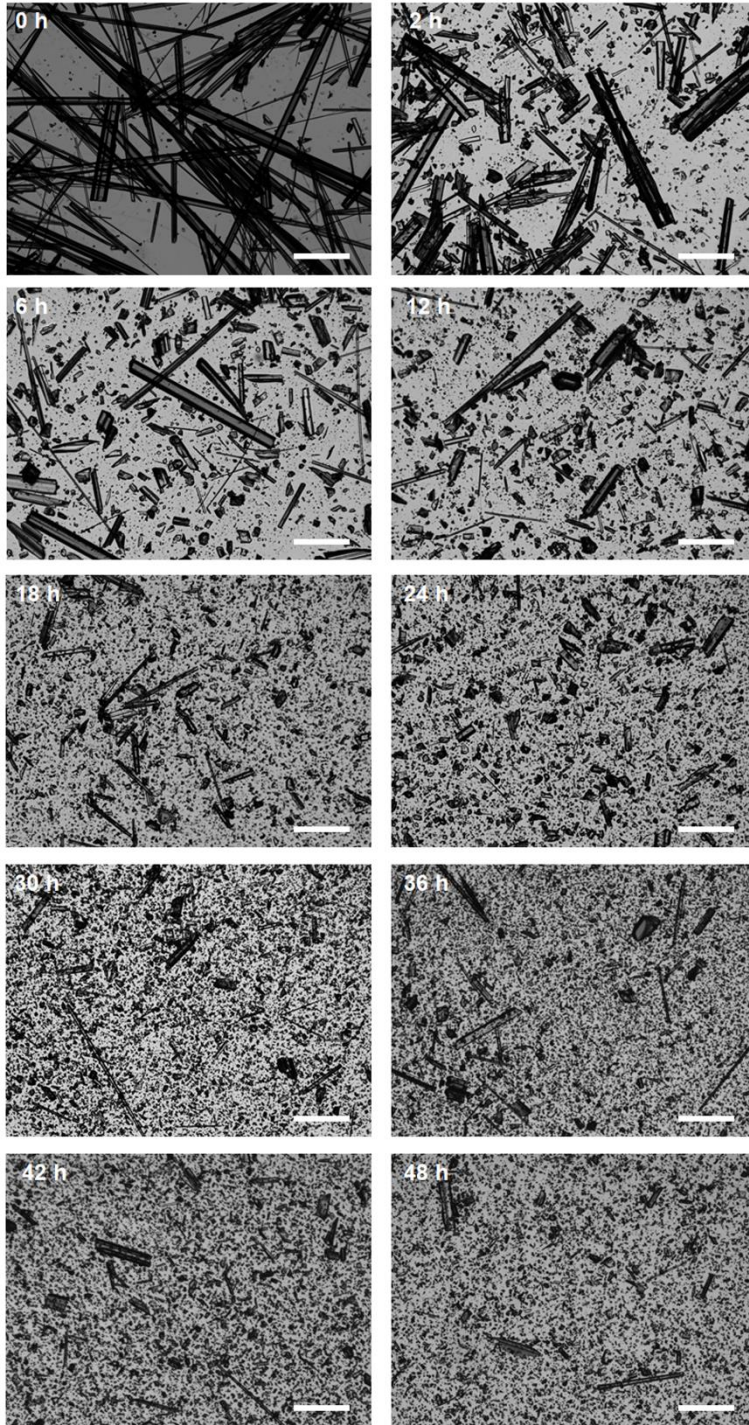
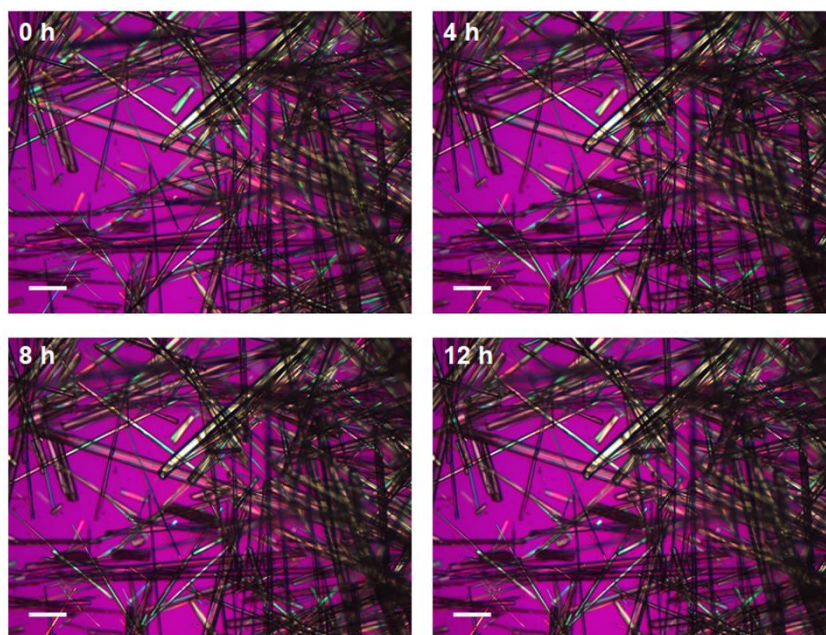


Fig. S6 Schematic representation of the experimental procedure for guest exchange. CBZ raw material (Form III) was first dissolved in hot toluene, followed by cooling to room temperature. After needle-like CBZ Form II (toluene) crystals were precipitated, appropriate amounts of PTHF ($C_{\text{PTHF}} = 12 \text{ mg/mL}$) was added and agitation was applied to initiate the guest exchange.

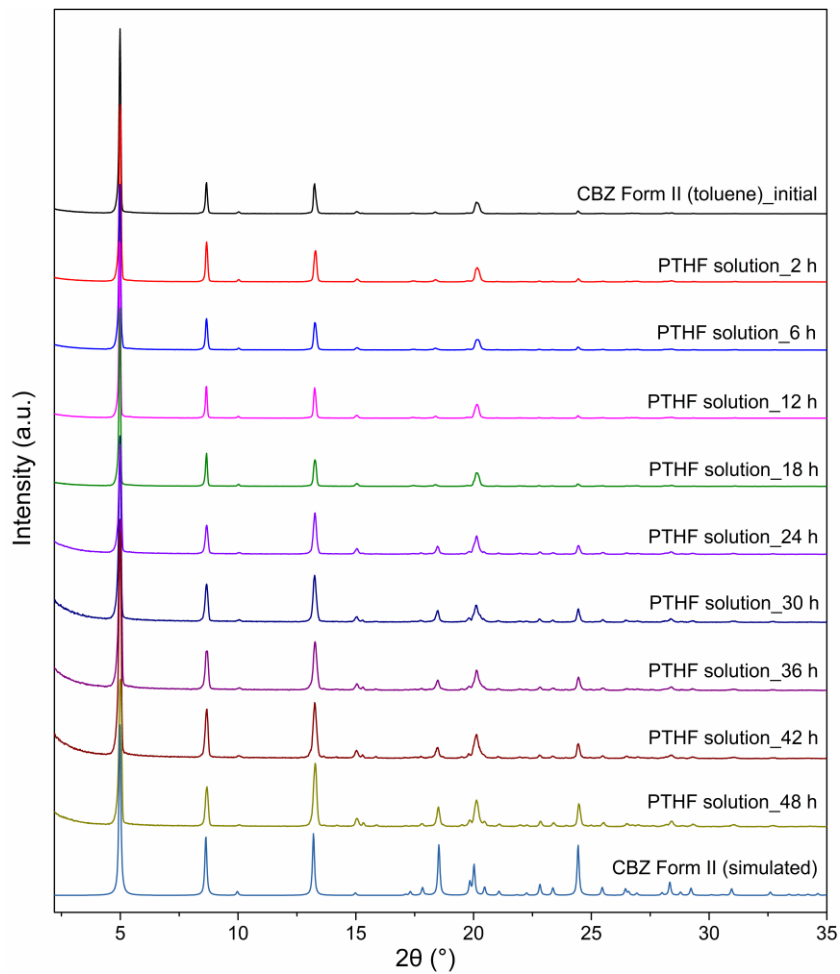


(a)

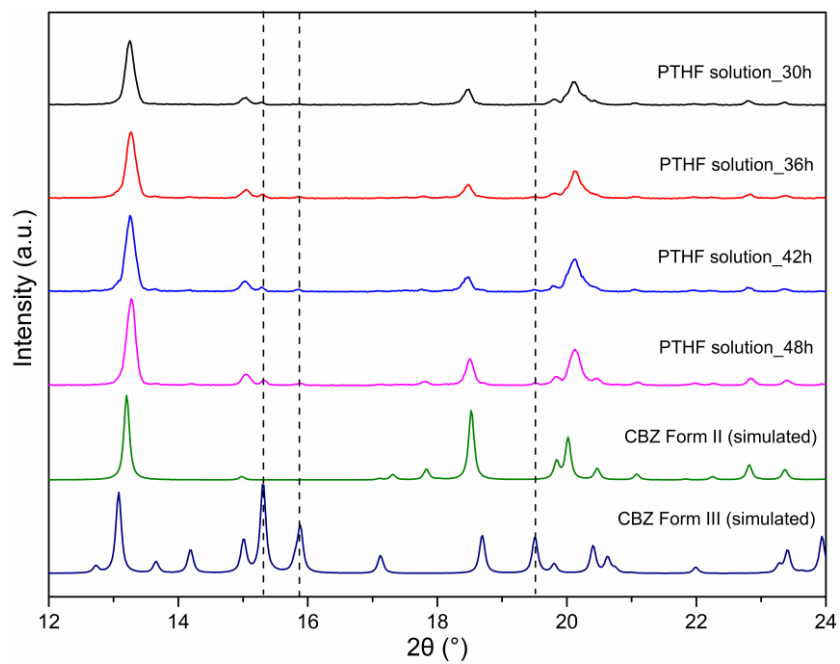


(b)

Fig. S7 (a) POM images of the guest exchange experiments (initial $C_{\text{PTHF}} = 12 \text{ mg/mL}$) with stirring. The crystal morphology gradually changed with time. The initial needle-like crystals broke apart and smaller crystals formed. (b) POM images of CBZ Form II (toluene) in toluene solution (initial $C_{\text{PTHF}} = 12 \text{ mg/mL}$) without stirring. No crystal morphology changes were observed even after 12 h. The bars represent $200 \mu\text{m}$.



(a)



(b)

Fig. S8 (a) PXR D patterns of the CBZ crystals isolated from the guest exchange experiment (initial

$C_{\text{PTHF}} = 12 \text{ mg/mL}$) at different time intervals. The diffraction peaks characteristic of CBZ Form II remained almost unchanged for up to 48 h. (b) Very small amounts of CBZ Form III can be observed after 30 h (characteristic peaks are marked by the black dashed lines)

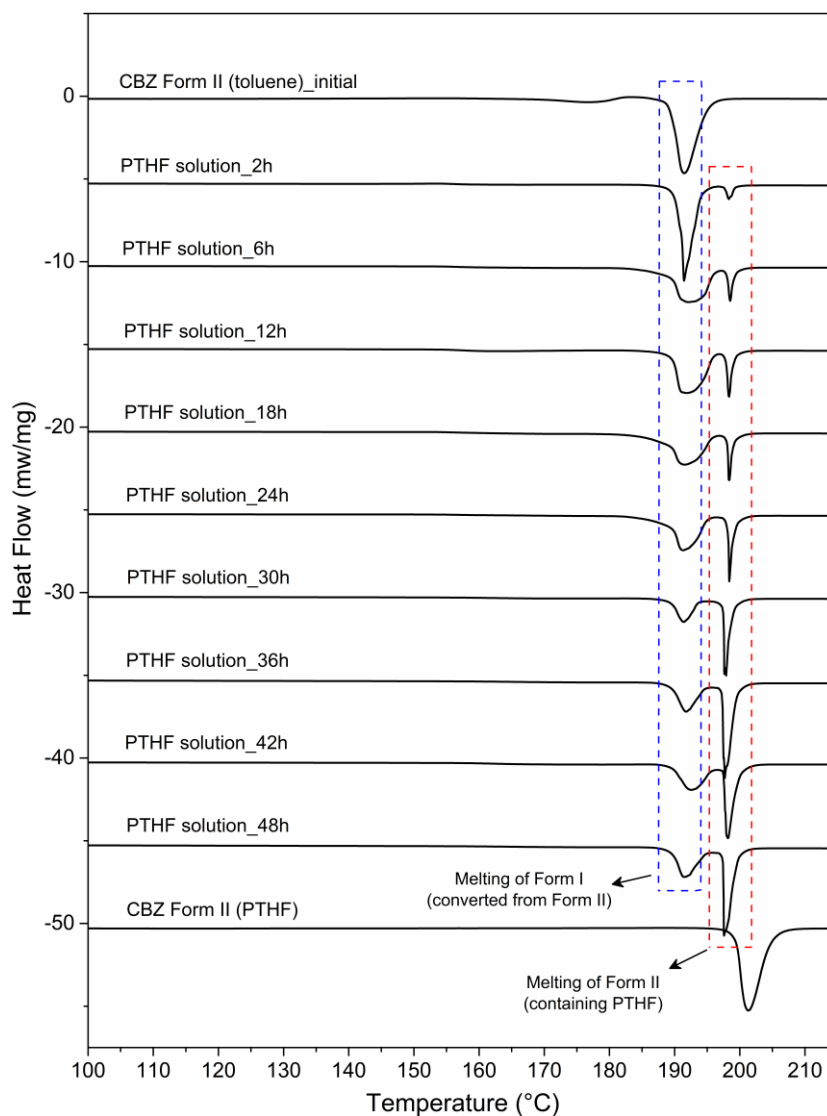


Fig. S9 DSC thermograms of the CBZ crystals isolated from the guest exchange experiment (initial $C_{\text{PTHF}} = 12 \text{ mg/mL}$) at different time intervals. In addition to the melting endotherm of CBZ Form I converted from CBZ Form II (toluene), a new endotherm appeared at $\sim 198 \text{ }^\circ\text{C}$ corresponding to the melting of CBZ Form II containing PTHF.

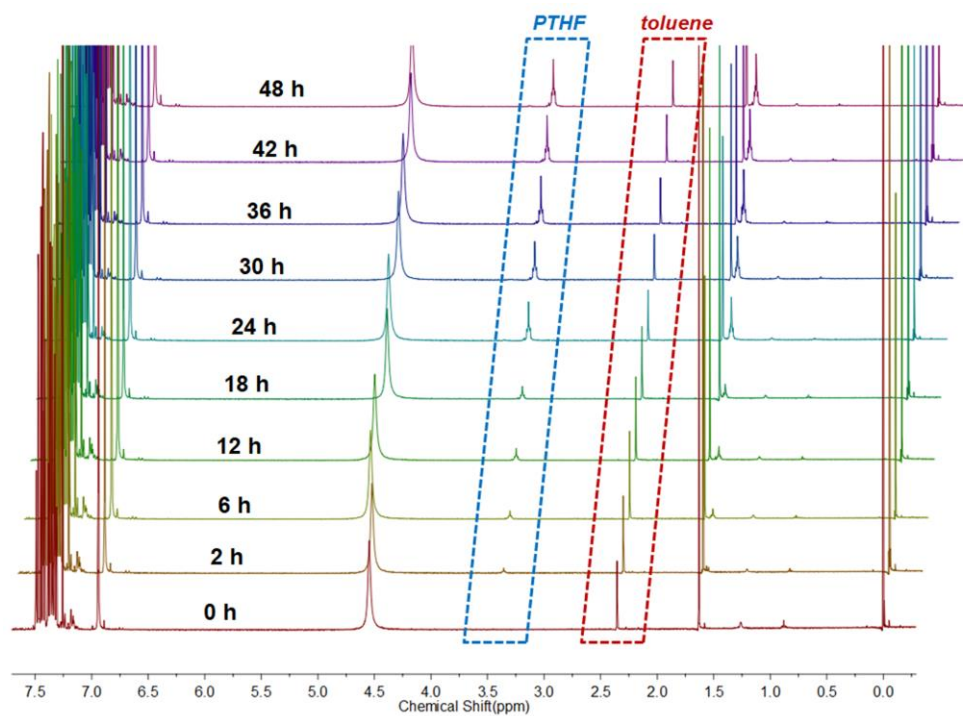


Fig. S10 ¹H-NMR spectra of the CBZ crystals isolated from the guest exchange experiments (initial $C_{\text{PTHF}} = 12 \text{ mg/mL}$) at different time intervals. The intensities of the proton signals characteristic of PTHF increased with time, while that of toluene showed the opposite trend.

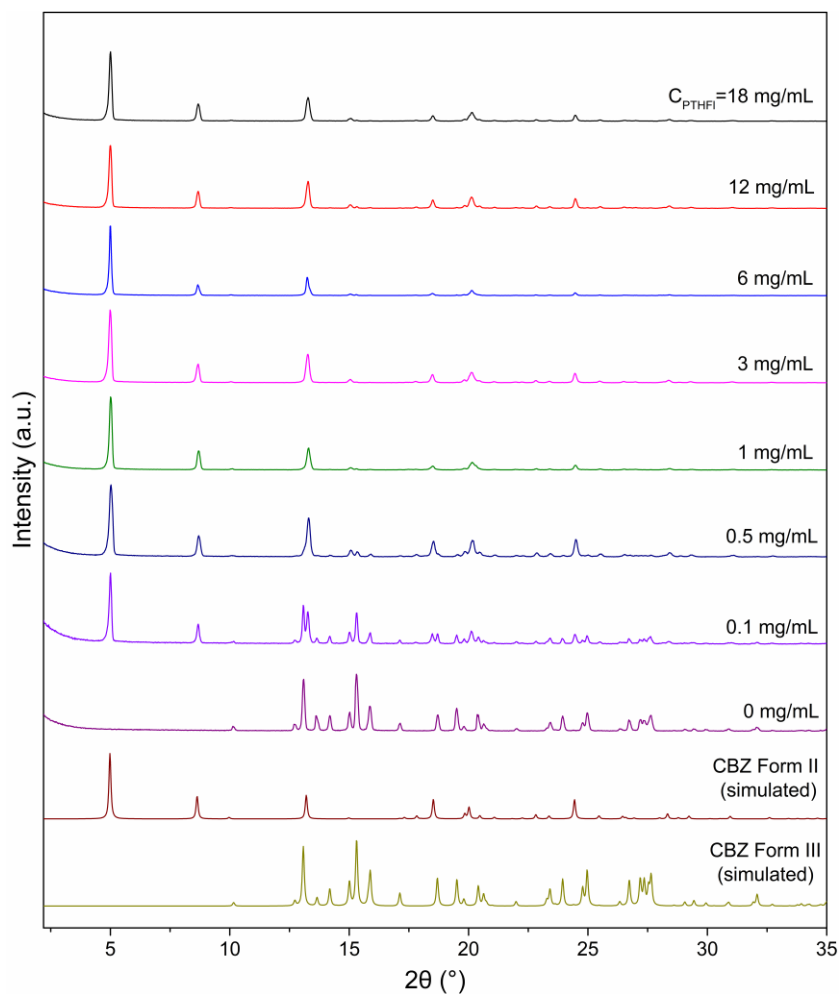


Fig. S11 PXR D patterns of the CBZ crystals isolated from the guest exchange experiments (with different initial PTHF concentrations) at 48 h. With $C_{\text{PTHF}} \geq 1$ mg/mL, the channel structure characteristic of CBZ Form II retained for at least 48 h. In contrast, noticeable CBZ Form III was observed at 48 h when $C_{\text{PTHF}} < 1$ mg/mL.

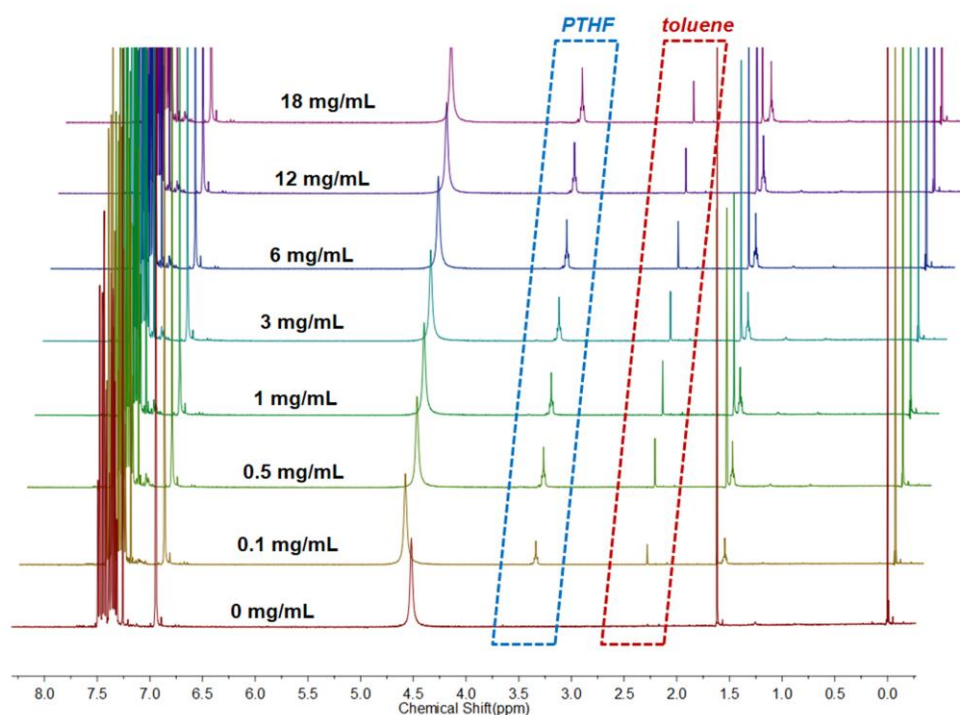


Fig. S12 ¹H-NMR spectra of the CBZ crystals isolated from the guest exchange experiments (with different initial PTHF concentrations) at 48 h.

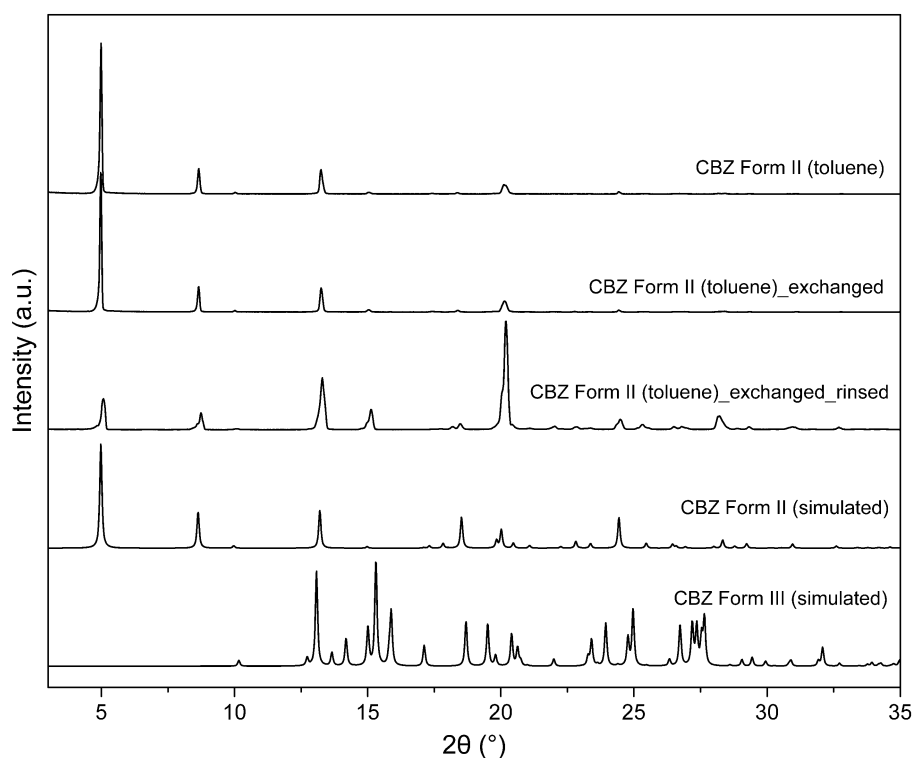


Fig. S13 PXRD patterns (from top to bottom): initial CBZ Form II (toluene); guest-exchanged CBZ Form II (initial $C_{\text{PTHF}} = 12$ mg/mL); guest-exchanged CBZ Form II after rinsing with EtOAc; calculated CBZ Form II and Form III. The channel structure characteristic of CBZ Form II was maintained after rinsing, however the relative intensities of the diffraction peaks showed changes

likely due to the variation in preferred orientation.

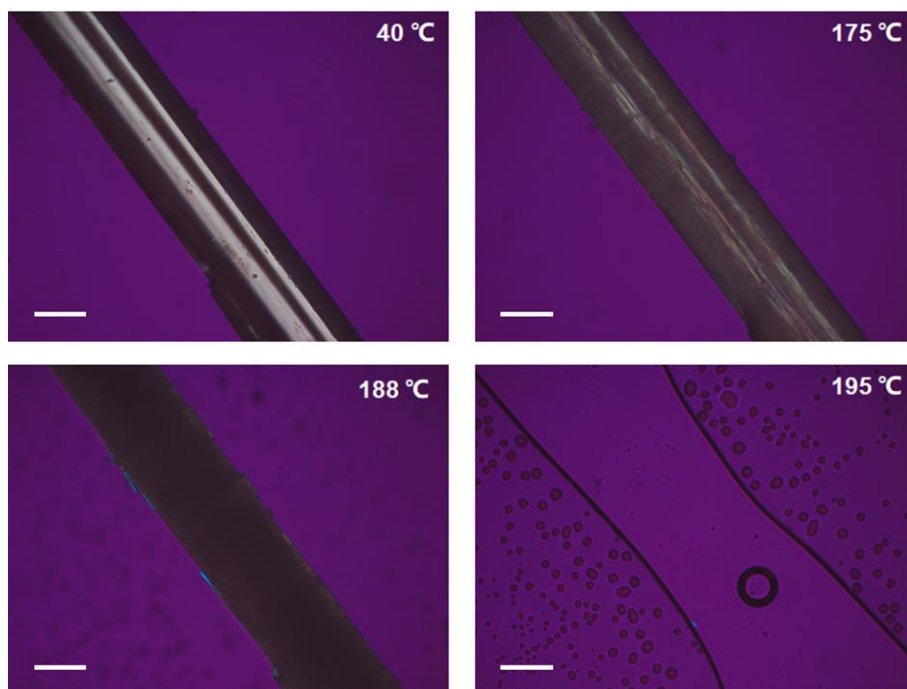


Fig. S14 Hot-stage POM images of the initial CBZ Form II (toluene) at a heating rate of 10 °C/min. Crystal darkening was observed during heating followed by a melting process. The bars represent 50 μm .

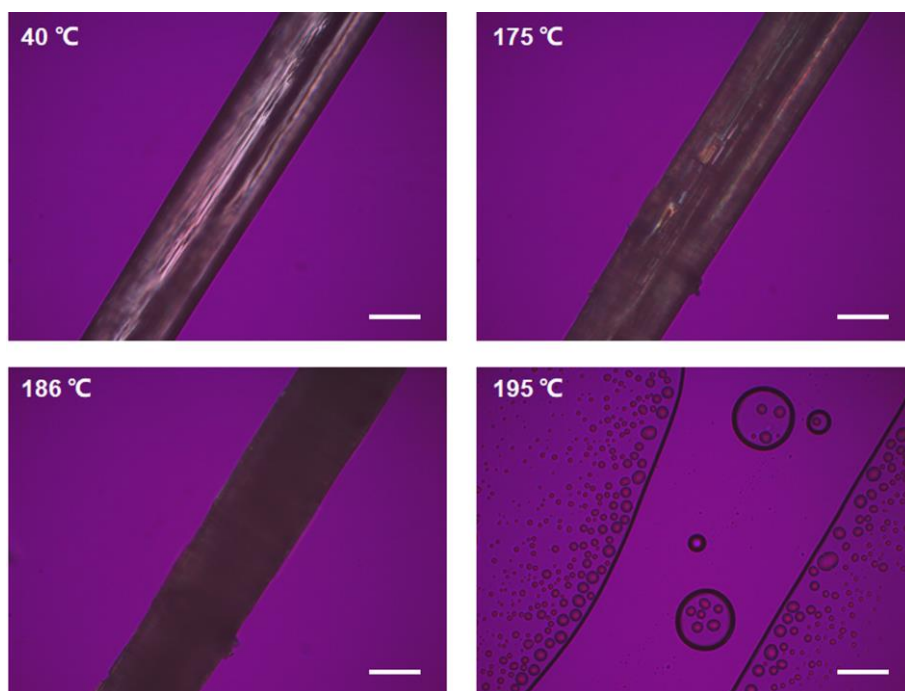


Fig. S15 Hot-stage POM images of the guest-exchanged and rinsed CBZ Form II at a heating rate of 10 °C/min. Crystal darkening was observed during heating followed by a melting process, similar

to that observed for the initial CBZ Form II (toluene). The bars represent 50 μm .

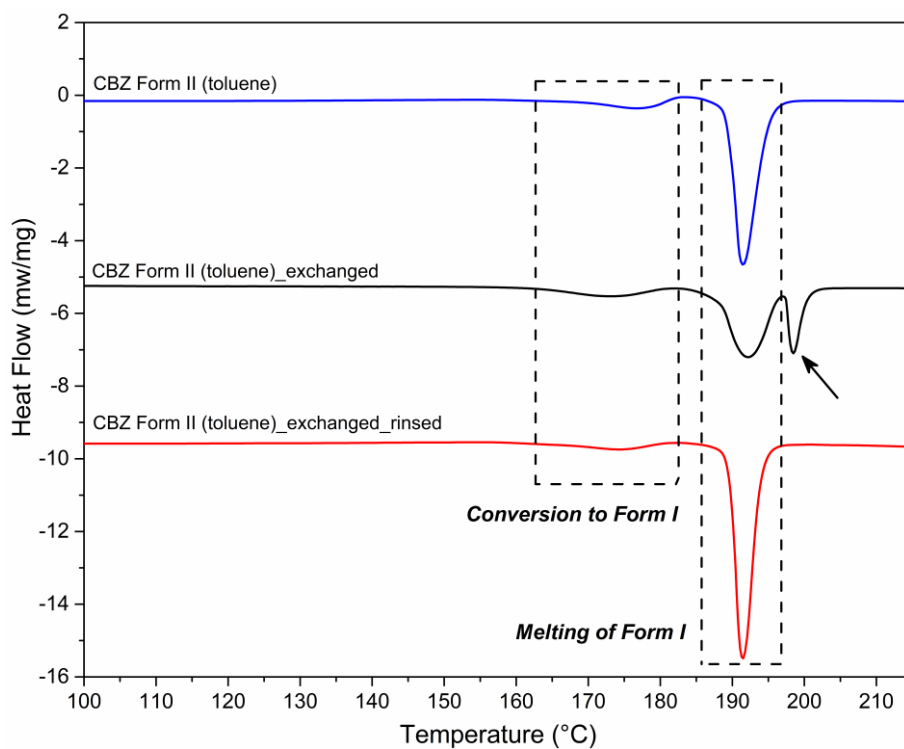


Fig. S16 DSC thermograms of CBZ Form II crystals (from top to bottom): initial CBZ Form II (toluene); guest-exchanged CBZ Form II (initial $C_{\text{PTHF}} = 12 \text{ mg/mL}$); guest-exchanged CBZ Form II after rinsing with EtOAc. The endotherm ($\sim 198 \text{ }^{\circ}\text{C}$) characteristic of the CBZ Form II containing PTHF could only be observed for the guest-exchanged CBZ Form II crystals.

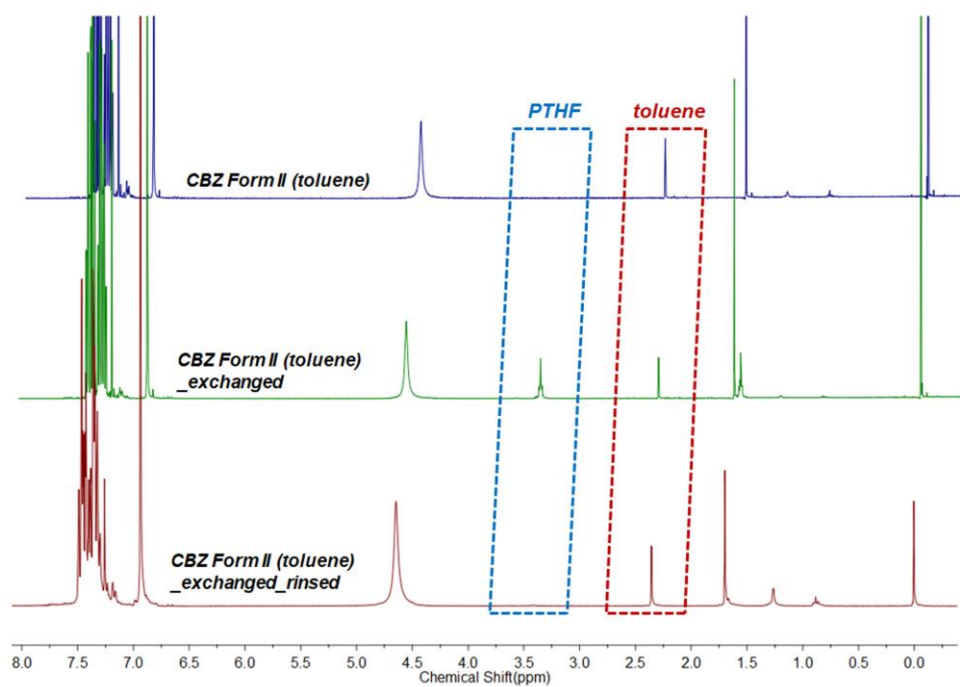


Fig. S17 ¹H-NMR spectra of CBZ Form II crystals (from top to bottom): initial CBZ Form II (toluene); guest-exchanged CBZ Form II (initial $C_{\text{PTHF}} = 12$ mg/mL); guest-exchanged CBZ Form II after EtOAc rinsing. The proton signals characteristic of PTHF could only be observed for the guest-exchanged CBZ Form II crystals.

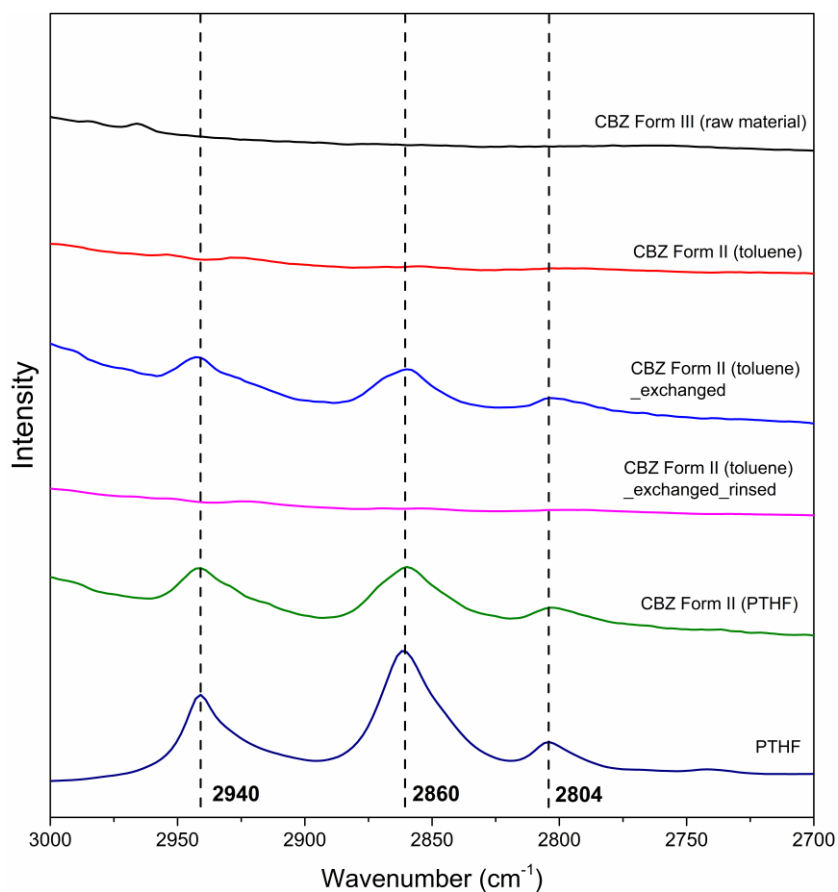


Fig. S18 ATR-FTIR spectra (from top to bottom): CBZ Form III (raw material); initial CBZ Form II (toluene); guest-exchanged CBZ Form II (initial $C_{\text{PTHF}} = 12 \text{ mg/mL}$); guest-exchanged CBZ Form II after rinsing with EtOAc; CBZ Form II (PTHF); PTHF raw material. The dashed lines indicate the characteristic stretching vibrations of CH_2 groups on PTHF chains.^{1,2} The IR absorption at 2940 cm^{-1} corresponds to asymmetric stretching vibration of the CH_2 groups not linked to the oxygen atoms. The IR absorption at 2860 cm^{-1} and 2804 cm^{-1} arises from the asymmetric and symmetric stretching vibrations of the CH_2 groups linked to the oxygen atoms, respectively

Table S1. ^1H T_1 and $T_{1\rho}$ values of CBZ Form II (PTHF), CBZ Form III and PTHF bulk crystals.

Sample	Relaxation Type	Integral region or peak (ppm)	Relaxation Time
CBZ Form II	^1H T_1 (s)	161.928-155.862	7.196 (0.028)
		144.809-137.800	7.169 (0.017)
		129.577-126.882	7.433 (0.072)
		126.882-121.220	7.165 (0.035)
		74.717-71.077	8.084 (0.144)
		29.022-25.517	7.294 (0.104)
	^1H $T_{1\rho}$ (ms)	159.097	17.075 (0.276)
		141.170	16.887 (0.364)
		127.825	16.290 (0.394)
		126.073	16.610 (0.547)
CBZ Form III	^1H T_1 (s)	73.099	19.337 (0.275)
		27.674	18.313 (0.504)
		161.254-155.727	300.873 (9.080)
		142.248-138.204	291.192 (3.154)
	^1H $T_{1\rho}$ (ms)	130.117-127.690	340.782 (24.414)
		127.690-124.051	309.264 (1.465)
		160.715-156.266	7.482 (0.112)
		141.574-138.743	13.591 (0.315)
PTHF	^1H T_1 (s)	130.117-127.690	15.400 (0.239)
		127.690-124.455	13.088 (0.660)
	^1H $T_{1\rho}$ (ms)	73.435-71.419	1.248 (0.002)
		30.745-25.117	1.242 (0.002)
		74.519-71.334	8.033 (0.462)
		30.172-25.387	9.370 (0.552)

References

- 1 K. Imada, T. Miyakawa, Y. Chatani, H. Tadokoro and S. Murahashi, *Makromol. Chem.*, 1965, **83**,

113-128.

2 K. Imada, H. Tadokoro, A. Umehara and S. Murahash, *J. Chem. Phys.*, 1965, **42**, 2807-2816.